

ANL/XFD/CP-92042
CONF-970706--

**HIGH RESOLUTION MONOCHROMATOR FOR INELASTIC SCATTERING
STUDIES OF HIGH ENERGY PHONONS USING UNDULATOR RADIATION
AT THE ADVANCED PHOTON SOURCE***

A. T. Macrander, M. Schwoerer-Böhning, P. M. Abbamonte, and M. Hu
*Experimental Facilities Division
Advanced Photon Source, Argonne National Laboratory
Argonne, IL 60439*

RECEIVED

AUG 26 1997

OSTI

August 1997

The submitted manuscript has been created by the University of Chicago as Operator of Argonne National Laboratory ("Argonne") under Contract No. W-31-109-ENG-38 with the U.S. Department of Energy. The U.S. Government retains for itself, and others acting on its behalf, a paid-up, nonexclusive, irrevocable worldwide license in said article to reproduce, prepare derivative works, distribute copies to the public, and perform publicly and display publicly, by or on behalf of the Government.

DISTRIBUTION OF THIS DOCUMENT IS UNLIMITED

MASTER

To be presented at the SPIE 42nd Annual Mtg., Conference Crystal/Bragg Optics for Synchrotron Radiation Beamlines, San Diego, CA, July 27- August 1, 1997, and published in the Proceedings.

*This work is supported by the U.S. Department of Energy, Basic Energy Sciences-Materials Sciences, under contract #W-31-109-ENG-38.

DISCLAIMER

**Portions of this document may be illegible
in electronic image products. Images are
produced from the best available original
document.**

DISCLAIMER

This report was prepared as an account of work sponsored by an agency of the United States Government. Neither the United States Government nor any agency thereof, nor any of their employees, makes any warranty, express or implied, or assumes any legal liability or responsibility for the accuracy, completeness, or usefulness of any information, apparatus, product, or process disclosed, or represents that its use would not infringe privately owned rights. Reference herein to any specific commercial product, process, or service by trade name, trademark, manufacturer, or otherwise does not necessarily constitute or imply its endorsement, recommendation, or favoring by the United States Government or any agency thereof. The views and opinions of authors expressed herein do not necessarily state or reflect those of the United States Government or any agency thereof.

High resolution monochromator for inelastic scattering studies of high energy phonons using undulator radiation at the Advanced Photon Source

A. T. Macrander, M. Schwoerer-Böhning, P.M. Abbamonte, M. Hu

Advanced Photon Source, Argonne National Laboratory
9700 South Cass Ave., Argonne, IL 60439

ABSTRACT

A monochromator for use at 13.84 keV with a calculated bandpass of 5.2 meV was designed, built, and tested. Tuning was performed by rotating the inner crystal of a pair of nested silicon channel-cut crystals. The inner crystal employs the (884) reflection, and the outer crystal employs a collimating asymmetric (422) reflection (dynamical asymmetry factor, b , equal to -17.5). Tests were done with a double-crystal Si(111) pre-monochromator situated upstream of the high resolution monochromator and a Si(777) backscattering crystal situated downstream. For this optical arrangement an ideal value of 6.3 meV as calculated by x-ray dynamical diffraction theory applies for the FWHM of the convolution of the net monochromator reflectivity function with that of the Si(777) reflection. This calculated value is to be compared to the value of 7.1 meV measured by tuning the high resolution monochromator. Measured efficiencies were less than ideal by a factor of 3.2 to 4.9, where the larger flux reduction factors were found with higher positron storage ring currents.

Keywords: X-ray monochromator, synchrotron radiation, high resolution, inelastic x-ray scattering

1. INTRODUCTION

Inelastic x-ray scattering experiments with a resolution sufficient for the study of phonons is a new field that has arisen due to the availability of synchrotron radiation.¹ Because of the low scattering cross section, very high incident beam fluxes with bandpasses of the order of $\Delta E/E = 10^{-7}$ are needed. Access to such beams is becoming increasingly available at both the European Synchrotron Radiation Facility (ESRF)² and at the Advanced Photon Source (APS). Both the pioneering instrument called INELAX (see ref. 1) at the synchrotron in Hamburg (HASYLAB) and the more recent instrument at ESRF³ have employed a backscattering geometry to reach the requisite incident bandpass. Energy scanning with such a backscattering monochromator (BSM) is achieved by tuning the temperature difference between the monochromator and a high

resolution analyzer. ⁴ Beamline layouts with a BSM are made complicated i) because of the need to transport the beam close to a sample before diffracting it from the BSM and ii) because measurements of the energy transfer require energy scanning of all intervening energies between the elastic peak and an inelastic peak. This is undesirable for spectra of excitations having large energy transfers because of difficulties in ascertaining the zero of energy, i.e., the temperature of the elastic peak may drift over long time spans. Because the present monochromator may be scanned rapidly from an elastic peak to the elastic peak, this drift is reduced. The inelastic scattering beamline in the Synchrotron Radiation Instrumentation Collaborative Access Team (SRI-CAT) of the APS has instead employed in-line monochromators to set a narrow bandpass. Four-reflection monochromators with one channel-cut crystal nested inside another and employing an asymmetric reflection for the outer channel-cut crystal were developed for use at 14.4 keV, ⁵ the nuclear resonance energy of ⁵⁷Fe, and have proven useful for the measurement of the phonon density of states of samples containing ⁵⁷Fe. ⁶ We have designed, built, and tested such a nested monochromator for use at 13.84 keV for the purpose of performing momentum resolved phonon studies employing a backscattering analyzer using the Si(777) reflection.

2. HIGH RESOLUTION MONOCHROMATOR

The optical arrangement of nesting two channel-cut crystals with an asymmetric reflection for the outer channel-cut crystal was introduced by Ishikawa et al.⁷ High energy resolution is achieved by means of two mechanisms: i) collimation and ii) backscattering. A collimating first reflection is followed by a high order second reflection having a large Bragg angle. The second reflection should be as close to backscattering as is practicable. These two effects both serve to reduce the geometrical contribution to the resolution given by:

$$\left(\frac{\Delta E}{E}\right)_{\text{geometrical}} = \frac{\Delta\theta}{\tan\theta}$$

as applied to the inner crystal. Increased collimation after the first reflection reduces $\Delta\theta$ and the high Bragg angle of the inner reflection increases $\tan\theta$.

For use at 13.84 keV, the backscattering energy for the Si(777) reflection, we chose the (422) reflection for the outer channel cut and the (884) reflection for the inner channel cut. A beam path diagram for this combination is shown in Fig. 1, detailed parameters are listed in Table I, and a photograph of the crystals is shown in Fig. 2.

Crystals were cut from (111) oriented boules that were 100 mm in diameter and were grown by the float zone technique. A Meyer-Burger⁸ slicing saw with a diamond impregnated bronze blade suitable for rapid cutting, i.e., with large diamond particles, was used to cut both crystals. Long diffraction faces for both channel cuts were present after sawing, and these were ground by hand to a fine finish using 9 micron aluminum oxide grit. The long diffracting faces of the inner crystal were then shortened using a grinding wheel. Acid etching of the entire crystals for strain removal was then performed in a mixture of nitric acid and hydrofluoric acid. After etching was done, polishing of the diffraction surfaces was performed by hand in three sequential steps: i) with 3 micron diamond slurry, ii) with 1 micron diamond slurry, and iii) with a colloidal suspension of 0.05 micron silica to provide both chemical as well as abrasive polishing action.

3. EXPERIMENTAL RESULTS AND DYNAMICAL DIFFRACTION CALCULATIONS

Tests were performed at beamline 3-ID of the APS in the optical configuration shown in Fig. 3. We used radiation from the first harmonic of an undulator. A pre-monochromator was used to absorb the large heat load presented by the undulator for which we used a (+,-) double-crystal arrangement of two Si(111) crystals.⁹ For energy analysis, we employed backscattering from a Si(777) reflection at a Bragg angle of 89.95 deg into a p-i-n detector. Data for this arrangement are shown in Fig. 4. The energy was tuned by rotating the (884) inner crystal. The energy change upon a rotation by $\Delta\phi$ is not simply obtained from Bragg's law for the (884) crystal alone. Rather, the dispersive configuration of the high resolution monochromator implies the following relationship:

$$\frac{\Delta E}{E} = \frac{\Delta\phi}{(\tan\theta_{422} + \tan\theta_{884})},$$

which yields a value of 1.881 meV/microrad for $\Delta E/\Delta\phi$. We note that this is not at a fixed exit operation. However, the change in exit angle is very small (3 microradian per 100 meV) as is evident from Fig. 5, and the change in exit height is also quite small (0.5 micron per 100 meV). We monitored the temperature of both crystals (they were placed in air) and measured a small temperature rise of the outer crystal after opening the shutter. Monochromator alignments were performed only after the temperature was stabilized.

Dynamical x-ray diffraction calculations for this optical arrangement have been performed. A "Diamond diagram"¹⁰ applicable either just before or just after the high resolution monochromator is shown in Fig. 5. Such a diagram shows lines representing the $y=\pm 1$ values of a Darwin curve, where y is a reduced variable that can be converted to either angle or energy.¹¹ The slope of the (884) related lines in this diagram (corresponding to the derivative of Bragg's law) is reduced by a factor of 17.5 due to the asymmetry of the (422) reflection. This reduction factor accounts for the collimation. A low inherent slope (to which the reduction factor is applied) is obtained due to the large Bragg angle of the (884) reflection, namely 81.8 deg. A full calculation of the reflectivity for 6 reflections (2 from the pre-monochromator and 4 from the high resolution monochromator) is shown in Fig. 6. Here Darwin curves¹² at different energies were obtained by shifting them according to Bragg's law for each reflection. Explicit inclusion of refraction was not necessary because all crystals were aligned to be at $y=0$. The structure-factor-related polarization terms in the dielectric constant of the crystals are listed in Table II. We incorporated the Hönl corrections for anomalous dispersion ($\Delta f'$ and $\Delta f''$) according to data by Cromer and Liberman¹³ (as made available by Brennan and Cowan¹⁴) and Debye-Waller factors according to Deutsch et al.¹⁵

A cross cut at constant angle through the surface shown in Fig. 6 is shown in Fig. 7. We note the profile is decidedly non-Gaussian with quite steep sides. The FWHM of this cross cut is 5.2 meV. We find that cross cuts at other angles in Fig. 6 are not dispersed in energy, i.e., the FWHM pertaining to the angle-integrated energy distributions corresponding to Fig. 6 is also 5.2 meV. A convolution of the surface in Fig. 6 with a Si(777) reflectivity function was also performed and is shown in Fig. 4. A value of 6.3 meV is found to apply for the FWHM of this final distribution which

represents a simulation of our experiment, and, as shown in Fig. 4, is to be compared to a value of 7.1 meV for the FWHM of the data. The data were obtained with a storage ring current of 80 mA for one block of a diced sandwich-style analyzer as detailed by Schwoerer-Böhning et al. (see ref. 4).

The dynamical diffraction theory value for the FWHM of the Si(777) reflection itself is 5.0 meV. We note that the quadrature addition of 5.0 and 5.2 meV for the net width yields a calculated value of 7.2 meV, and that this value is too large by 0.9 meV. This is expected due to the non-Gaussian nature of the dynamical diffraction profiles.

A main concern for such monochromators is the efficiency. Ideally, one desires to reduce the throughput by a factor proportional only to the bandpass reduction. For radiation distributions with vertical divergence's less than or equal to the acceptance of the (422) reflection (26.7 microrad), the ideal throughput reduction ratio is 1000 as calculated by dynamical diffraction. At larger divergences, this ratio increases significantly because the more divergent rays are not accepted by the (422) reflection. Values for the loss ratio have been measured and ranged from 3200 to 4900 depending on the positron current in the storage ring. The loss ratio was measured with ion chambers placed immediately upstream and immediately downstream of the high resolution monochromator. The downstream ion chamber chamber had been calibrated to the upstream one by letting the beam pass directly from one to the other, i.e., without intervening optics. The reason for the loss in throughput beyond that expected from an ideal performance has yet to be clarified. Excess loss can have resulted not only from an increased divergence of the beam incident on the high resolution monochromator owing to an imperfect performance of the pre-monochromator but also from less than perfect alignment of the Bragg planes on the opposite sides of the (422) and (884) channel-cut crystals.

ACKNOWLEDGMENTS

We are indebted to V. Kushnir for assistance and to the SRI CAT staff of sector 3 at the APS for the performance of the beamline. We are also indebted to the management of the APS, the Experimental Facilities Division, and the SRI CAT for their support. This work supported by the U.S. Department of Energy, Basic Energy Sciences, under Contract no. W-31-109-ENG-38.

FIGURE CAPTIONS

- 1) Cross-sectional view of the high resolution monochromator crystals showing the optical beam path. Beveled edges on the crystals were made parallel to the (422) and (884) Bragg planes.
- 2) High resolution monochromator crystals.
- 3) Optical layout used to make measurements at the APS.
- 4) **Data points:** experimental results obtained by rotating the inner channel-cut crystal. The FWHM is 7.1 meV.

Solid line: results of dynamical diffraction calculations simulating the experiment. The ordinate values were normalized to the data. The FWHM is 6.3 meV.

5) Dumond diagram applicable either before or after the high resolution monochromator.

6) The calculated reflectivity function for the high resolution monochromator and including the pre-monochromator. The surface represents the distribution in angle and energy for a beam exiting the high resolution monochromator.

7) Cross cut at zero angle through the monochromator reflectivity function. The FWHM is 5.2 meV.

¹ E. Burkel, *Inelastic Scattering of X-rays with High Energy Resolution*, Springer-Verlag, New York, 1991.

² F. Sette, G. Ruocco, M. Krisch, U. Bergmann, C. Masciovecchio, G. Signorelli, R. Verbeni, *Phys. Rev. Lett.* **75**, pp. 850-853, 1995.

³ R. Verbeni, F. Sette, M.H. Krisch, U. Bergmann, B. Gorges, C. Halcoussis, K. Martel, C. Maschiovecchio, J.F. Ribois, G. Ruoco, and H. Sinn, *J. Synchrotron Rad.* **3**, pp. 62-64, 1996.

⁴ For analyzer results obtained at the APS, see M. Schwoerer-Böhning, P.M. Abbamonte, A.T. Macrander, and V.I. Kushnir, these proceedings; for analyzers used at INELAX, see ref. 1; for analyzers used at the ESRF, see C. Masciovecchio, U. Bergmann, M. Krisch, G. Ruocco, F. Sette, and R. Verbeni, *Nucl. Instrumen. Meth.* **B111**, pp. 181-186, 1996.

⁵ T.Toellner, T. Mooney, S. Shastri, E.E. Alp, *SPIE Proceedings Vol. 1740*, pp. 218-223, 1992; T.M. Mooney, T. Toellner, W. Sturhahn, E.E. Alp, and S.D. Shastri, *Nucl. Instrum. Meth.* **A347**, pp. 348-351, 1994; T. Toellner, Ph.D. Thesis, Northwestern Univ., June 1996.

⁶ M. Seto, Y. Yoda, S. Kikuta, X.W. Zhang, and M. Ando, *Phys. Rev. Lett.* **74**, pp. 3828-3831, 1995; W. Sturhahn, T.S. Toellner, E.E. Alp, X. Zhang, M. Ando, Y. Yoda, S. Kikuta, M. Seto, C.W. Kimball, and B. Dabrowski, *Phys. Rev. Lett.* **74**, pp. 3832-3835, .

⁷ T. Ishikawa, Y. Yoda, K. Izumi, C.K. Suzuki, X.W. Zhang, M. Ando, and S. Kikuta, *Rev. Sci. Instrum.* **63**, pp. 1015-1018, 1992.

⁸ Meyer-Burger AG, Maschinenfabrik, CH-3613 Steffisburg, Switzerland.

⁹ L. Assoufid, K.W. Quast, and H.L.T. Nian, *SPIE Proceedings Vol. 2855*, pp. 250-261, 1996.

¹⁰ J.W. Dumond, *Phys. Rev.* **52**, pp. 872-883, 1937.

¹¹ W.H. Zachariasen, *Theory of X-ray Diffraction in Crystals*, p.123, Dover, New York, 1967.

¹² H. Cole and N.R. Stemple, *J. Appl. Phys.* **33**, pp. 2227-2233, 1962.

¹³ D.T. Cromer and D.A. Liberman, *Acta Crystallogr.* **A37**, p. 267- , 1981.

¹⁴ S. Brennan and P.L. Cowan, *Rev. Sci. Instrum.* **63**, pp. 850-853, 1992.

¹⁵ M. Deutsch, M. Hart, and P. Sommer-Larsen, *Phys. Rev.* **B40**, pp.11666-11669, 1989.

Table I. Parameters for the (422) x (884) high resolution monochromator for 13.84 keV.

Outer crystal:

Bragg reflection	(422)
Bragg angle	23.8°
Darwin width	6.4 microrad
Asymmetry angle	21.5°
Angle of incidence	2.3°
Dynamical b factor	-17.5
Divergence accepted	26.7 microrad
Divergence outgoing	1.5 microrad

Inner crystal:

Bragg reflection	(884)
Bragg angle	81.8°
Darwin width	3.7 microrad
Asymmetry angle	60°
Angle of incidence	21.8°
Dynamical b factor	-1.7
Divergence accepted	2.8 microrad
Divergence outgoing	4.8 microrad

Table II. Crystal polarization terms (proportional to the structure factor) for the dielectric constant of silicon.

$$\Psi'_{111} = -2.678 \times 10^{-6}$$

$$\Psi''_{111} = -2.865 \times 10^{-8}$$

$$\Psi'_{422} = -2.236 \times 10^{-6}$$

$$\Psi''_{422} = -3.733 \times 10^{-8}$$

$$\Psi'_{884} = -4.971 \times 10^{-7}$$

$$\Psi''_{884} = -2.309 \times 10^{-8}$$

$$\Psi'_{777} = -3.933 \times 10^{-7}$$

$$\Psi''_{777} = -1.856 \times 10^{-8}$$

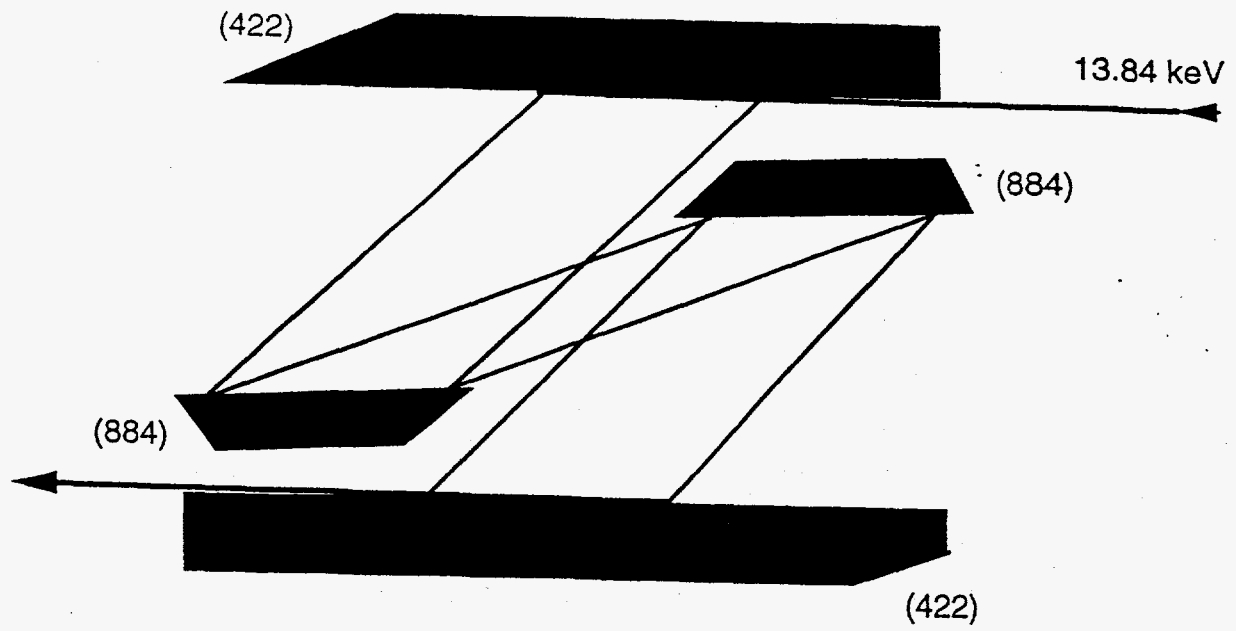
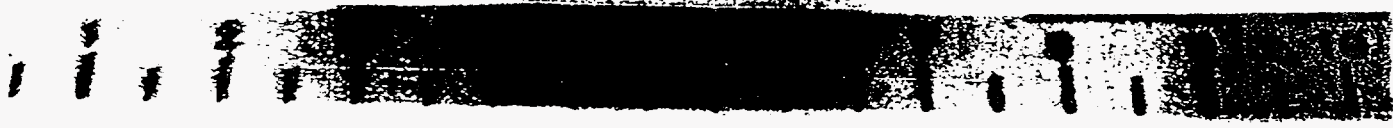
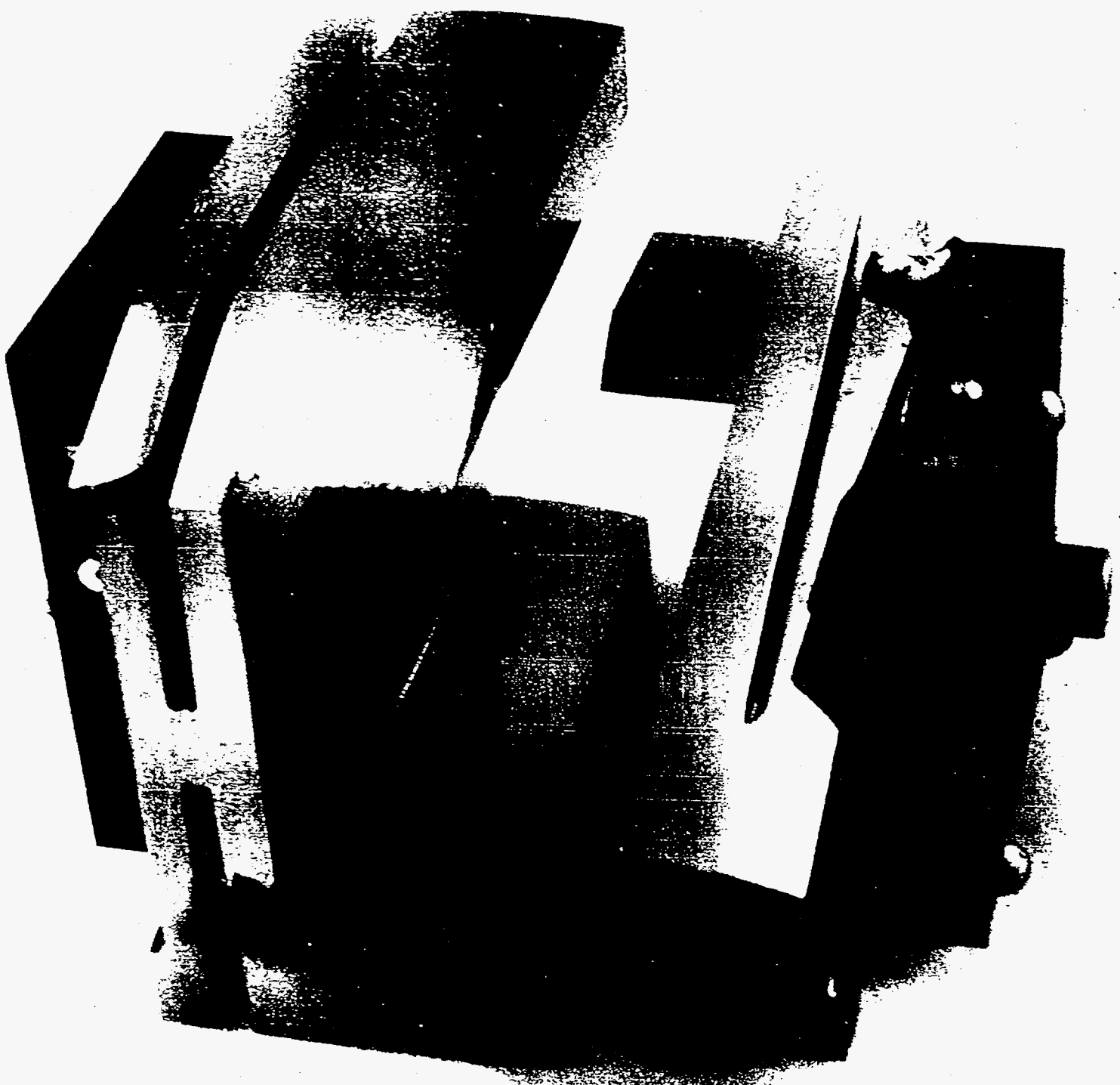


Fig. 1



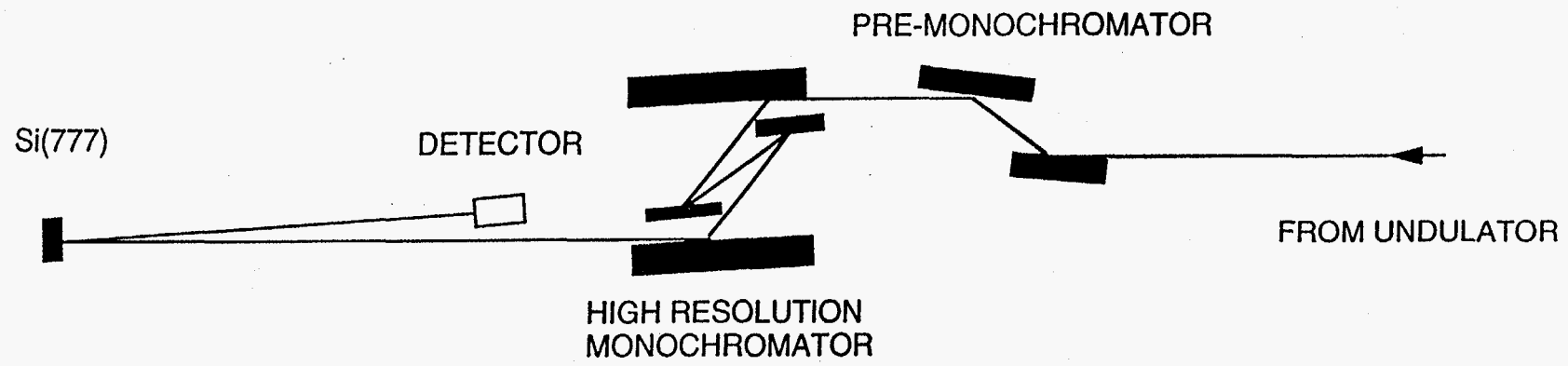


Fig. 3

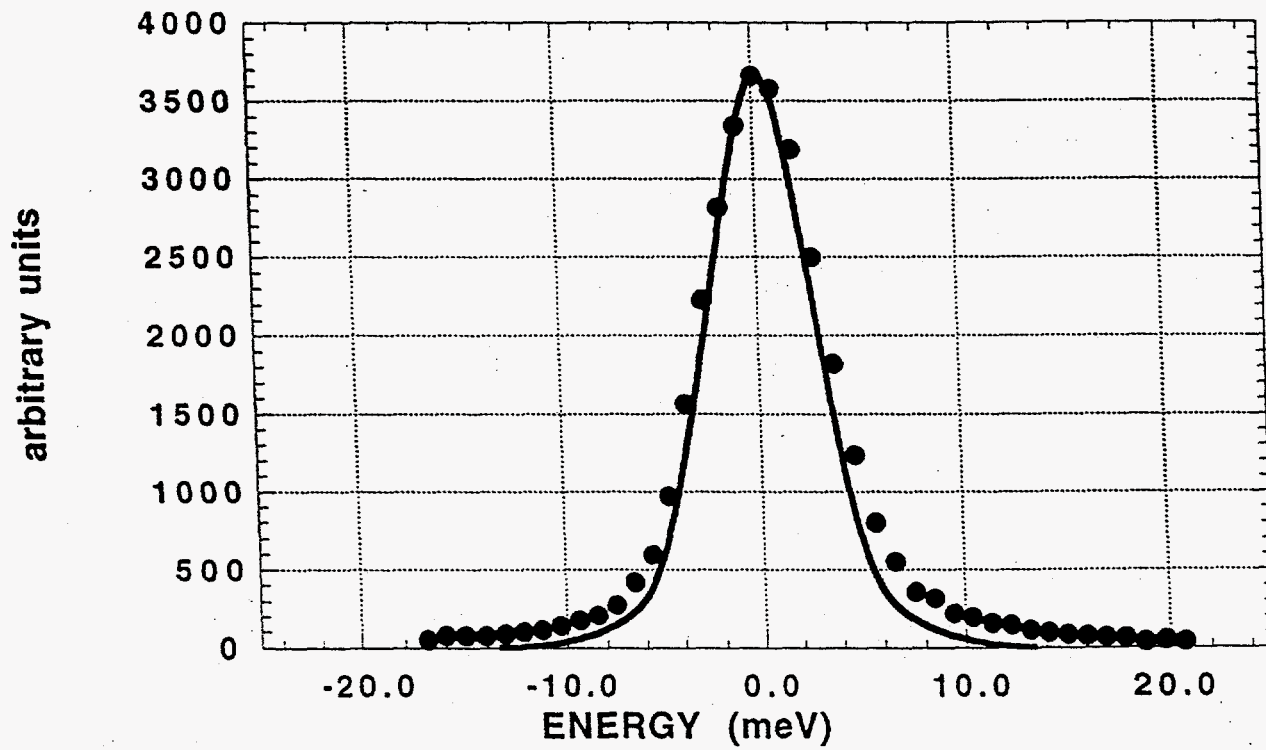


Fig.4

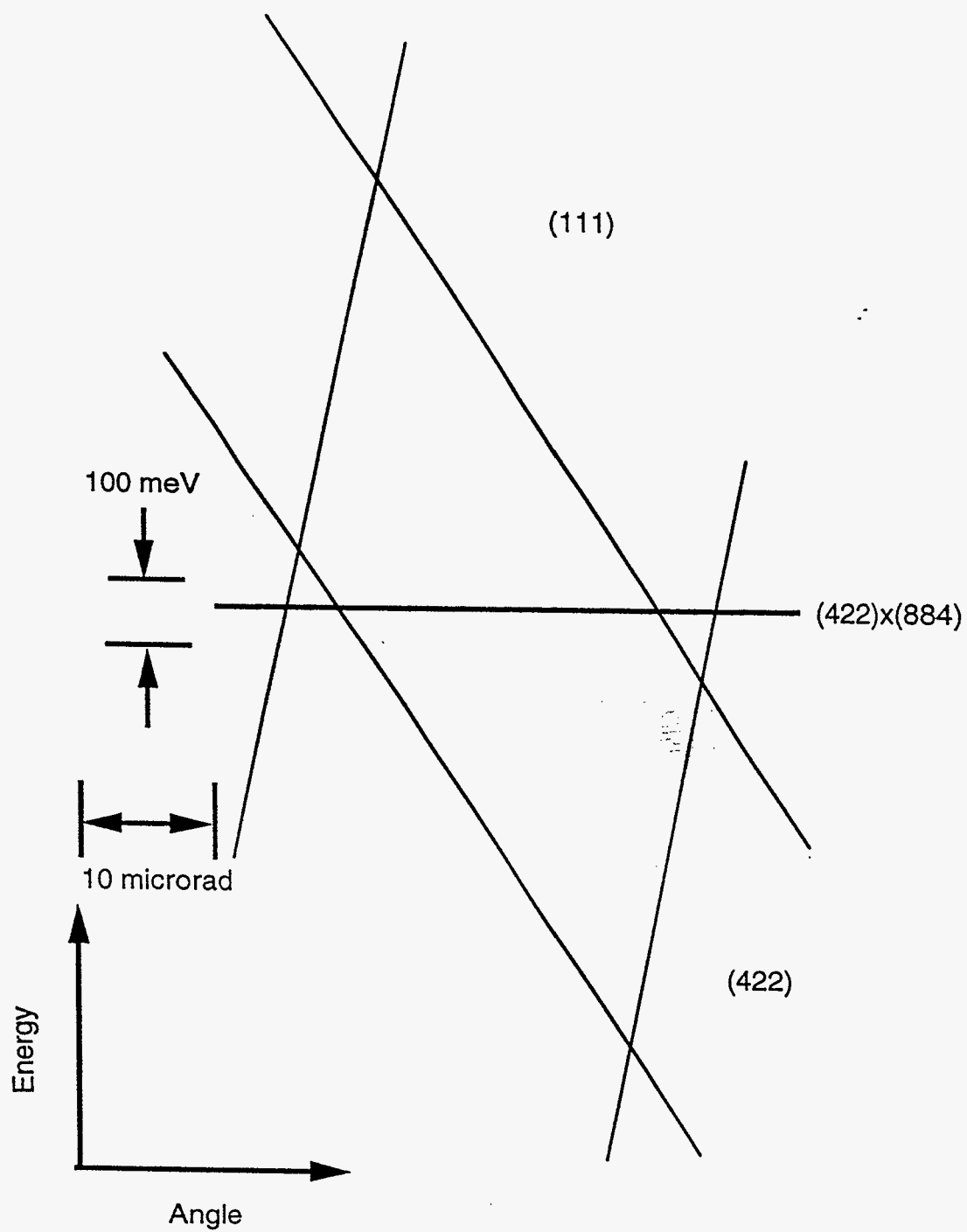


Fig. 5

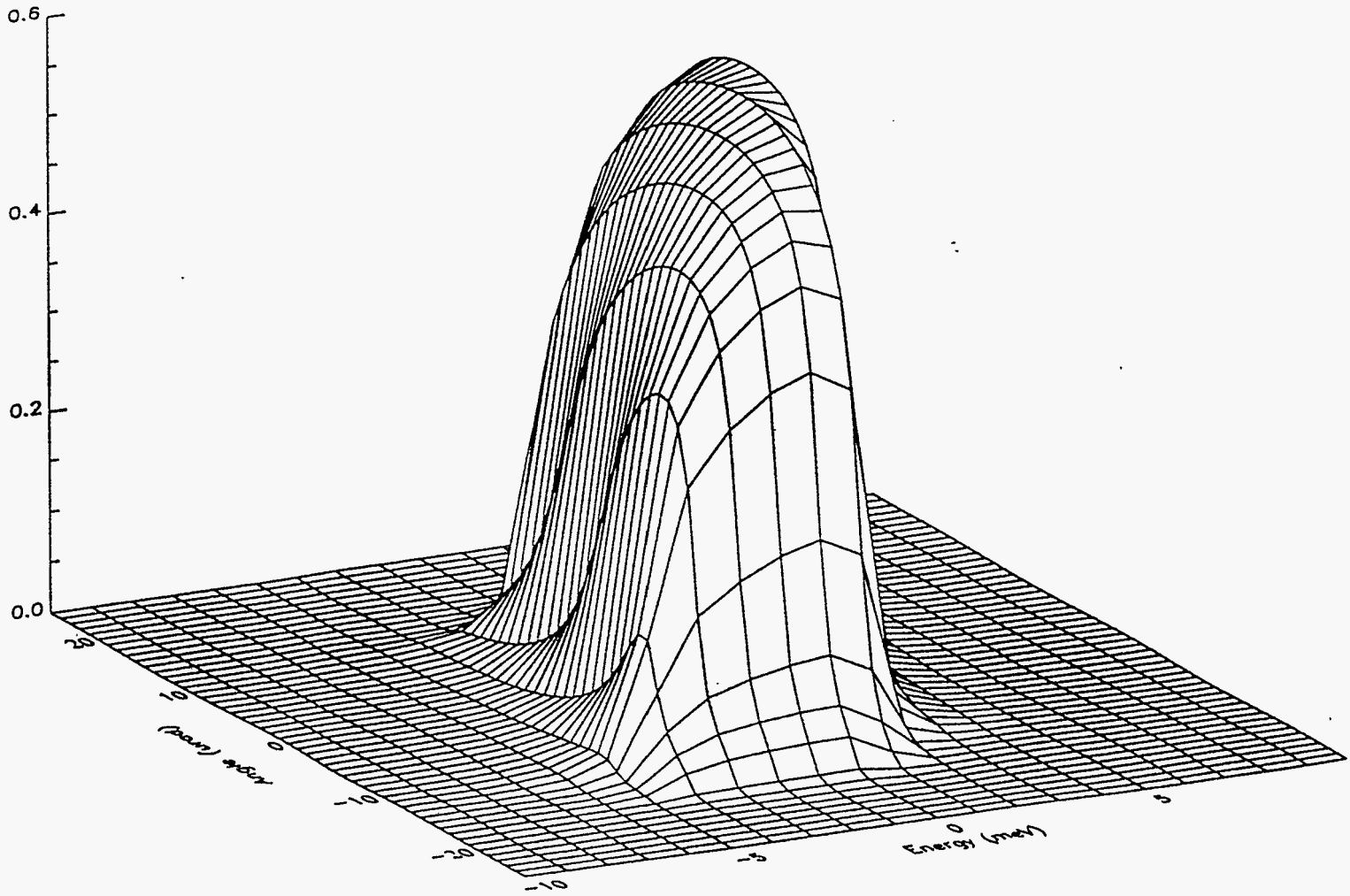


Fig. 6

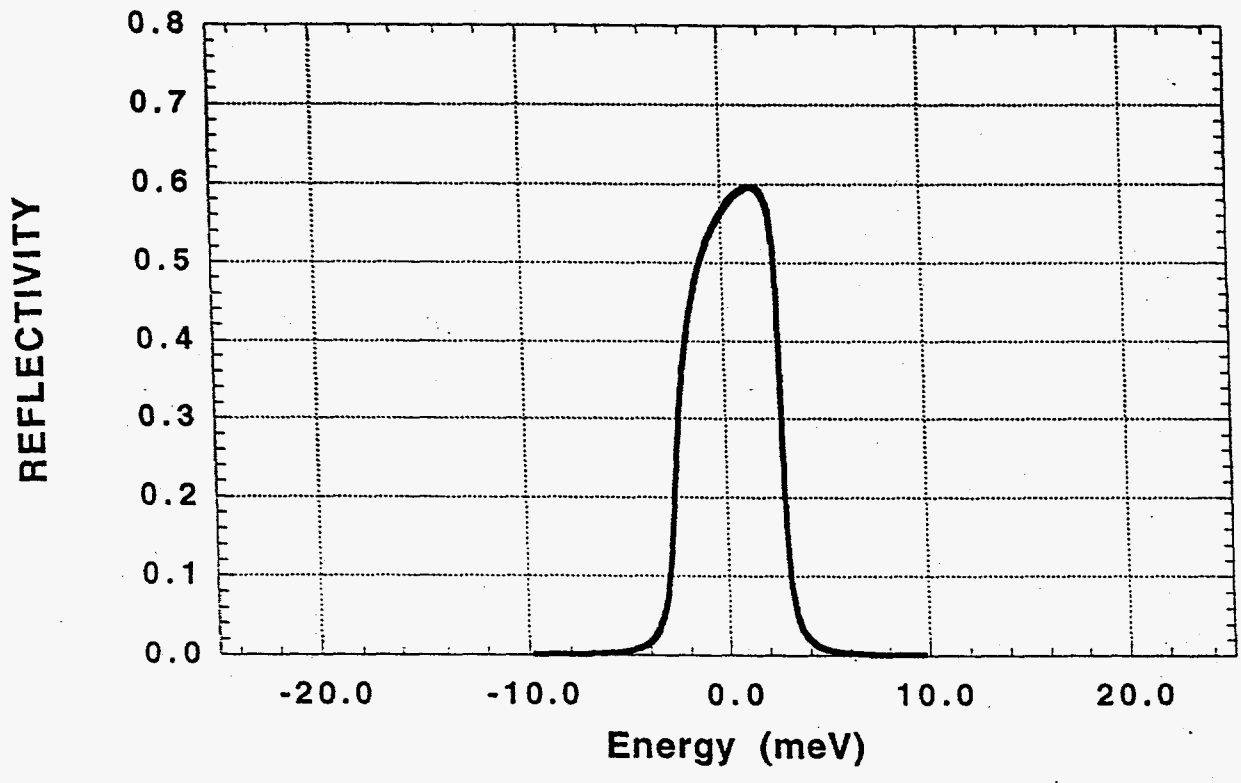


Fig. 7